Journal of
Applied
Crystallography
ISSN 0021-8898

Received 22 September 2006
Accepted 10 November 2006

Hydrostatic low-range pressure applications of the Paris–Edinburgh cell utilizing polymer gaskets for diffuse X-ray scattering measurements

Karena W. Chapman,[a]* Peter J. Chupas,[a] Charles A. Kurtz,[a] Darren R. Locke,[b] John B. Parise[b] and Joseph A. Hriljac[c]

[a]X-ray Science Division, Advanced Photon Source, Argonne National Laboratory, Argonne, IL 60439, USA, [b]Geosciences Department, Stony Brook University, Stony Brook, NY 11794-340, USA, and [c]School of Chemistry, University of Birmingham, UK. Correspondence e-mail: chapmank@aps.anl.gov

The use of a polymeric Torlon (polyamide–imide) gasket material in a Paris–Edinburgh pressure cell for *in situ* high-pressure X-ray scattering measurements is demonstrated. The relatively low bulk modulus of the gasket allows for fine control of the sample pressure over the range 0.01–0.42 GPa. The quality of the data obtained in this way is suitable for Bragg and pair distribution function analysis.

1. Introduction

The principal drive underlying many *in situ* high-pressure studies is the need to understand the materials that make up the Earth under conditions in which they are stable, typically above 2 GPa. However, many important phenomena in technologically relevant materials occur at more moderate pressures and, as such, the ability reliably to access less high pressure is valuable.

The Paris–Edinburgh (PE) pressure cell (Besson *et al.*, 1992; Klotz *et al.*, 2004) represents a robust compact easy-to-use large-volume pressure apparatus suitable for X-ray scattering structural studies. It generates pressure through compression of the sample, confined within a gasket, between a pair of anvils by means of a hydraulic pump. For a given gasket size, the physical properties of the gasket material largely limit the range of pressures accessible. At the upper bound, the gasket material extrudes and no longer keeps the anvils apart or the anvils themselves start to deform plastically. At the lower limit, the intrinsic strength of the gasket material must be overcome before controllable pressure is generated at the sample. The boron–epoxy composite routinely used as gaskets for X-ray scattering experiments with the PE cell (Mezouar *et al.*, 1999) allows access to pressures up to 4 GPa for gaskets of 10 mm diameter, and 7 and 18 GPa for 7 and 5 mm gaskets, respectively.

Here we demonstrate the viability of softer gasket materials (K = 3.3 GPa), used in combination with fluid pressure-transmitting media, to allow controlled access to lower, hydrostatic pressures for X-ray scattering measurements for Bragg and pair distribution function (PDF) analysis with sodium chloride used as both sample and internal pressure standard (Decker, 1971). Although diamond-anvil cells can also be utilized in this range, they are not always ideal for these types of experiments due to the large contribution of Compton scattering from the diamonds to the measured intensities and the comparatively small sample volume (Martin *et al.*, 2005).

2. Experimental methods

A gasket, of appropriate shape for use with anvils with 10 mm diameter conical indents (3.5 mm diameter sample cavity), was machined from commercially available Torlon 4503 rod. A manually pre-compressed NaCl pellet was loaded into the gasket, wet with fluid pressure-transmitting media (2-propanol) and sandwiched between anvils (tungsten carbide, WC, inserts) within a VX5 model PE cell. The anvils were covered with polyimide film to minimize contact with the fluid pressure-transmitting media.

The PE cell was mounted on the instrument at beamline 11-ID-B at the Advanced Photon Source, Argonne National Laboratory, with the incident (and scattered) beam directed through the gasket *via* the gap between the anvils (Fig. 1). High-energy X-rays (90.48 keV, λ = 0.1370 Å) were used in combination with a MAR-345 image-plate detector to record diffraction images (Chupas *et al.*, 2003).

For pressure calibration, data were collected at a sample-to-detector distance of 791.14 mm, at ambient pressure and as the applied pressure was increased at 10 (2) bar (1 MPa) intervals up to 100 bar (10 MPa). Raw images were processed using *Fit2D* (Hammersley, 1997; Hammersley *et al.*, 1996). The sample-to-detector distance was refined using a CeO_2 NIST standard. The lattice parameters were obtained from Rietveld refinement of a structural model for NaCl within *GSAS* (R_{wp} = 3.4–3.6%) (Larson & Von Dreele, 1987). The sample pressure was determined from the pressure-induced changes in cell volume based on a third-order Birch–Murnaghan equation of state for NaCl (K_0 = 23.5897 GPa and K_0' = 4.8206).

For PDF analysis at the maximum pressure, the sample-to-detector distance was decreased (232.12 mm) and higher-energy X-rays (126.8 keV, λ = 0.09778 Å) were used to collect data to high values of

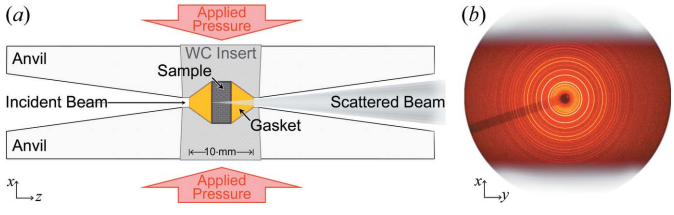

Figure 1
(*a*) A schematic representation of the sample environment in the PE cell and (*b*) a diffraction image collected at ambient pressure. The scattered beam is shadowed by the anvils in the x direction (horizontal).

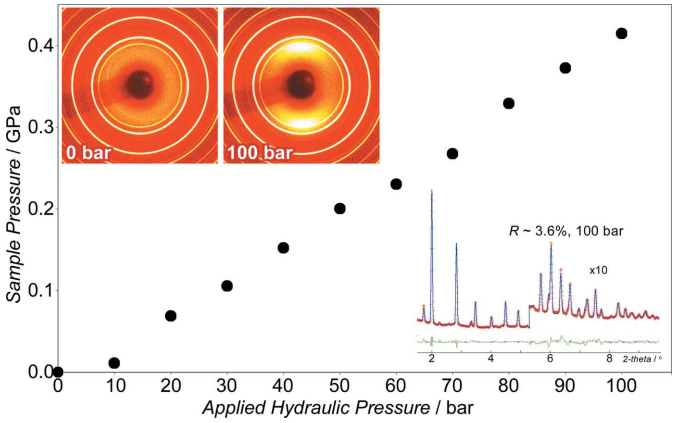

Figure 2
The sample pressures generated at various applied pressures. Low-angle diffraction images (top inset) show the diffraction texture which develops for the gasket. A representative Rietveld refinement profile is shown (inset).

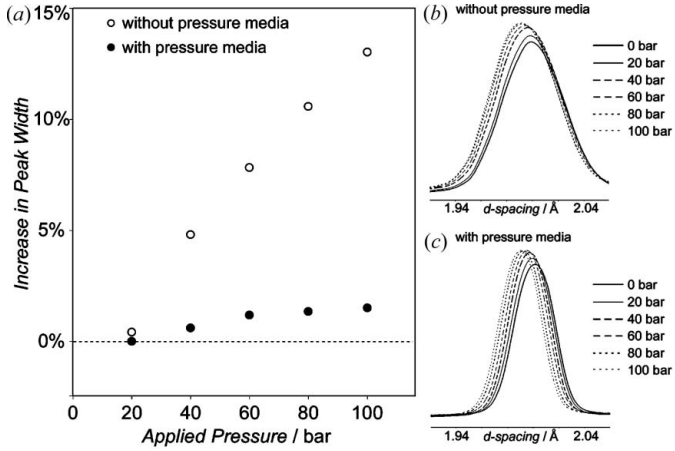

Figure 3
The pressure dependence of the 220 NaCl reflection (*a*), measured under non-hydrostatic (*b*) and near hydrostatic (*c*) conditions.

momentum transfer ($Q \simeq 17$ Å^{-1}). The PDF was extracted using *PDFgetX2* (Qiu *et al.*, 2004), subtracting the contributions from the sample environment and background to the measured diffraction intensity as measured by translating the PE cell such that X-rays were incident on the gasket only. Corrections for multiple scattering, X-ray polarization, sample absorption, and Compton scattering were then applied to obtain the structure function $S(Q)$. Direct Fourier transform of the reduced structure function $F(Q) = Q[S(Q) - 1]$ up to $Q_{max} \simeq 17$ Å^{-1} gave $G(r)$, the pair distribution function. Refinement of a model against $G(r)$ was performed within *PDFFIT* (Proffen & Billinge, 1999).

3. Results

Above 10 bar applied pressure, the Torlon gasket was sufficiently compressed to generate pressure at the sample. This corresponds to ~10% of the applied pressure required to generate pressure using the boron–epoxy gasket in an identical setup. The sample pressure increased with applied pressure at a rate of ~0.045 GPa per 10 bar (Fig. 2) until gasket failure at above 100 bar (0.042 GPa). In contrast to the near linear behavior observed here, the increase in sample pressure with the boron–epoxy gasket often decreases at higher pressures with plastic deformation of the anvils.

While no strain-texture was evident for the sample peaks, the development of diffraction texture at low angle along the direction of compression (x) was observed with increasing pressure (Fig. 2). This arose from strain-induced ordering in the gasket material (Gorlier *et al.*, 2001) and had minimal impact on the intensity in the perpendicular wedges of the image used to obtain the one-dimensional diffraction patterns.

Near hydrostatic conditions were maintained with the inclusion of alcohol-based fluid pressure-transmitting media. Under these conditions, the diffraction peaks from the sample shifted smoothly to shorter d-spacing with increasing pressure, with minimal broadening (Fig. 3). In contrast, data measured without pressure-transmitting media, with slightly different experimental conditions (lower resolution due to the shorter sample-to-detector distance and wavelength used), showed significant peak broadening upon application of pressure. At the pressures achieved with the Torlon gasket, it was not necessary to encapsulate the sample/fluid to prevent the anvil failure following contact with fluid seen at higher pressures (Marshall & Francis, 2002). Here, the anvils were covered to prevent this effect in

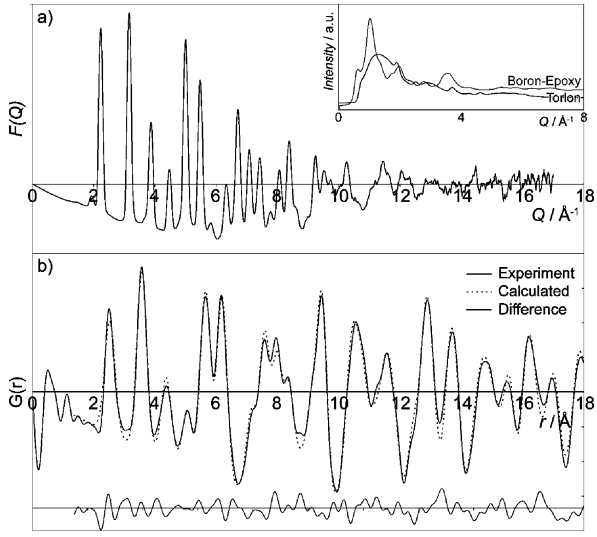

Figure 4
The reduced structure function [$F(Q)$, (*a*)] and the pair distribution function [$G(r)$, (*b*)] obtained for NaCl at 0.42 GPa. The scattering intensities from boron–epoxy and Torlon gaskets are shown (inset).

future higher pressure experiments. As Torlon is highly plastic, the fluid is reliably contained at low pressure without cracking, as often occurs for boron–epoxy. Alcohol odor evident in the recovered sample confirmed fluid containment during the experiment.

The reduced structure function and PDF for NaCl at pressure are shown in Fig. 4. The PDF calculated for the refined model of NaCl was in good agreement with the data (R = 0.1513). The contribution to the scattering from Torlon is smoother, less structured with lower intensity at high Q than that from boron–epoxy, and this aids in the accurate normalization of the data. The tolerance of the normalization to the neglected scattering from the pressure-transmitting media is presumably due its extremely weak contribution.

The use of smaller gaskets shifts the accessible pressure range to higher values, by factors of 2–4 for boron–epoxy. Similar gains are expected for Torlon gaskets such that pressures up to 0.8–1.6 GPa may be achieved. It may also be possible to vary the pressure range by using other gasket materials. Offline tests on Vespel SP-1 (polyimide, K = 2.4 GPa) gaskets indicates that they withstand ~60% of the maximum applied pressure tolerated by Torlon 4503.

Use of the Advanced Photon Source was supported by the US Department of Energy, Office of Science, Office of Basic Energy Sciences, under Contract No. DE-AC02-06CH113. The PE cell was purchased as part of the SNAP project supported by grant DE-FG02-03ER46085. JBP acknowledges support of the NSF through grant DMR-0452444.

References

Besson, J. M., Nelmes, R. J., Hamel, G., Loveday, J. S., Weill, G. & Hull, S. (1992). *Physica B*, **180**, 907–910.
Chupas, P. J., Qiu, X., Hanson, J. C., Lee, P. L., Grey, C. P. & Billinge, S. J. L. (2003). *J. Appl. Cryst.* **36**, 1342–1347.
Decker, D. L. (1971). *J. Appl. Phys.* **42**, 3239–3244.
Gorlier, E., Haudin, J. M. & Billon, N. (2001). *Polymer*, **42**, 9541–9549.
Hammersley, A. P. (1997). ESRF Internal Report ESRF97HA02T.
Hammersley, A. P., Svensson, S. O., Hanfland, M., Fitch, A. N. & Häusermann, D. (1996). *High Pressure Res.* **14**, 235–248.
Klotz, S., Hamel, G. & Frelat J. (2004). *High Pressure Res.* **24**, 219–223.
Larson, A. C. & Von Dreele, R. B. (1987). *GSAS*. Report No. LAUR-86-748. Los Alamos National Laboratory, Los Alamos, NM 87545, USA.
Marshall, G. W. & Francis, J. D. (2002). *J. Appl. Cryst.* **35**, 122–125.
Martin, C. D., Antao, S. M., Chupas, P. J., Lee, P. L., Shastri, S. D. & Parise, J. B. (2005). *Appl. Phys. Lett.* **86**, 061910/1–3.
Mezouar, M., Bihan, T. L., Libotte, H., Godec, Y. L. & Hausermann, D. (1999). *J. Synchrotron Rad.* **6**, 1115–1119.
Proffen, T. & Billinge, S. J. L. (1999). *J. Appl. Cryst.* **32**, 572–575.
Qiu, X., Thompson, J. W. & Billinge, S. J. L. (2004). *J. Appl. Cryst.* **37**, 678.